Petrology and petrogenesis of volcanic rocks from the Uegusukudake Formation in Kume-jima, central Ryukyu Arc

Petrology and petrogenesis of volcanic rocks from the Uegusukudake Formation in Kume-jima, central Ryukyu Arc

Hiroshi KITAGAWA*,**, Ryuichi SHINJO*, and Yuzo KATO*

*Department of Physics and Earth Sciences, University of the Ryukyus, Senbaru 1, Nishihara, Okinawa 903-0213, Japan

**Present address: Institute for Study of the Earth's Interior, Okayama University at Misasa, Tottori 682-0193, Japan

Abstract

Major and trace element concentrations and Sr and Nd isotopic ratios are presented for volcanic rocks from the Uegusukudake Formation (~3-2 Ma) in Kume-jima, central Ryukyu Arc, in order to understand the origin of varieties of erupted magmas. The Uegusukudake Formation is mainly composed of lavas and pyroclastic rocks with subordinate dikes. Volcanic rocks collected from lavas and dikes are grouped into four types based on their petrological characteristics: (1) picrite basalt (PB); (2) aphyric, tholeiitic basalt and basaltic andesite (A-TH); (3) porphyritic, tholeiitic basaltic andesite (P-TH); and (4) porphyritic, calc-alkaline basaltic andesite and andesite (CA), in ascending order. The PB sample is isotopically distinct in having significantly low $^{87}Sr/^{86}Sr$ (0.7035) and high $^{143}Nd/^{144}Nd$ (0.51290) compared with the other three types. The A-TH, P-TH, and CA types have similar isotopic compositions ($^{87}Sr/^{86}Sr$=0.7045-0.7054, $^{143}Nd/^{144}Nd$=0.51270-0.51284) and show rather coherent incompatible trace element patterns. These results suggest that the three types of magmas were derived from a similar source material, distinctive from the source of the PB magma. A slight difference in isotopic and trace element ratios (La/Sm and La/Yb) among the three types can be attributed to the different degree of contributions of crustal assimilation. Geochemical variations within the A-TH type rocks can be explained by fractional crystallization, and the variation of the CA type is considered to have resulted from internal hybridization within a single magma reservoir. For the variation of the P-TH type, plagioclase accumulation is inferred to have played a dominant role.

1. Introduction

Arc volcanic centers remain relatively fixed for substantial periods of time (a few kiloyears). However, volcanic rocks erupted in a close spatial proximity commonly have a wide range of chemical compositions including major and trace element and isotopic

Received: January 6, 2004

compositions. These geochemical diversities can be attributed to shallow-level (i.e. intracrustal) processes, including fractional crystallization, magma mixing, and crustal assimilation, and deep-level (i.e. mantle wedge) processes, such as magma generation itself (varying degree of partial melting). A characterization of these processes is important to understand the evolution of magmatic plumbing system beneath island arc.

In this paper, volcanic rocks from the late Pliocene Uegusukudake Formation in Kume-jima, central Ryukyu Arc, is studied. The Uegusukudake Formation is a good target for investigating magmatic processes beneath island arc, because volcanic rocks have a marked compositional diversity, including high-magnesian picrite basalt, low-magnesian tholeiitic rocks, and calc-alkaline andesite, and they erupted during the short period of time, approximately 2.8 to 2.1 Ma (Miki, 1995; Ito and Shiraki, 1999; Kitagawa and Shinjo, 2001). Although some geochemical data have been reported on volcanic rocks from the Uegusukudake Formation, these data are restricted to mafic rocks. Shinjo (1999) reported detailed geochemical data including Sr and Nd isotopic compositions of the PB rocks, and discussed their generation by linking with the high-magnesian andesite from O-jima, present just east of Kume-jima (Fig. 1). Ito and Shiraki (1999) also reported the petrological and mineralogical characteristics and the K-Ar age of the PB lava. But these two studies have been focused only on the PB lava. Shinjo et al. (1999) presented geochemical data for some mafic rocks excluding those of the PB type from the Uegusukudake Formation, in addition to the volcanic rocks from other fields in the Ryukyu Arc and the Okinawa Trough, in order to investigate the geochemical evolution of the source mantle beneath the Ryukyu Arc and the Okinawa Trough. However, there have been no detailed petrological and geochemical studies concerning the volcanic rocks from the whole Uegusukudake Formation. The purpose of this paper is to understand the generation of volcanic rocks from the Uegusukudake Formation, by evaluating the processes causing their chemical varieties, based on major, trace, and Sr-Nd isotopic compositions.

2. Geological Setting

The Ryukyu Arc is about 1200 km-long convergent margin extending from south Kyushu to Taiwan. It consists of three sub-arcs: northern, central, and southern Ryukyu Arcs, divided by the Tokara Strait and Kerama Gap, respectively. Kume-jima is located at about 90 km west of the Okinawa-jima in the central Ryukyu Arc and on the eastern margin of the Okinawa Trough, an active intra-continental back-arc basin (Fig. 1).

Volcanic rocks in Kume-jima occur in two formations: the middle Miocene Aradake Formation and late Pliocene Uegusukudake Formation. The Aradake Formation is distributed over the southeastern part of Kume-jima, and consists mainly of lavas and pyroclastic rocks of andesitic compositions (Shinjo and Kato, 1988). K-Ar ages of 17.7 and

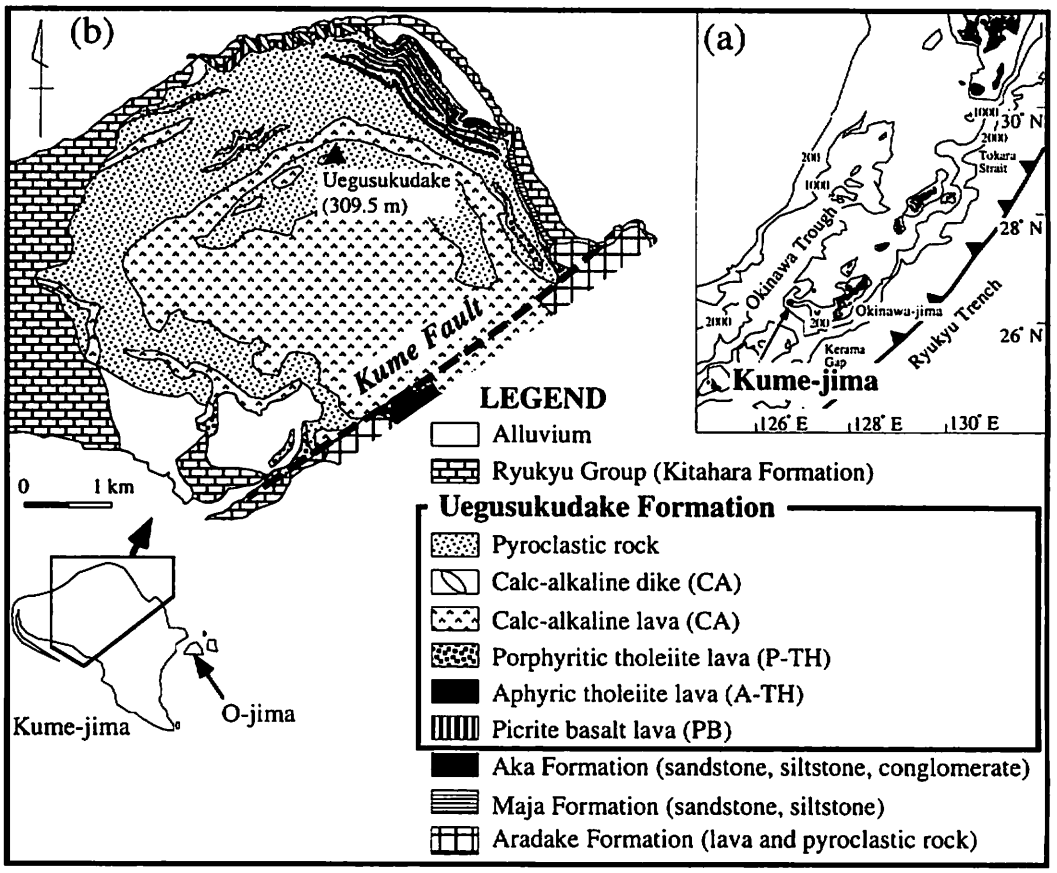

Figure 1. (a) Map of the Ryukyu Arc. Bathymetric contours (200, 1000 and 2000) are from Maritime Safety Agency of Japan (1991). (b) Geological map of the northwestern part of Kume-jima. The distribution of the Maja and Aka Formations are after Nakamura et al. (1999). K-Ar ages of volcanic rocks from the Uegusukudake Formation follow (1) Ito and Shiraki (1999), (2) Kitagawa and Shinjo (2001), and (3) Miki (1995).

12.6 Ma (Nakagawa and Murakami, 1975) and fission track ages of 12.8±2.1 and 15.1± 2.6 Ma (Daishi *et al.*, 1987) were obtained for the Aradake volcanic rocks. The Shimajiri Group, which unconformably overlies the Aradake Formation, consists of three formations: the late Miocene Maja Formation, late Pliocene Aka Formation, and Uegusukudake Formation (Nakamura *et al.*, 1999). The Maja and Aka Formations occur just southeast of the Kume Fault (Kato, 1985), and in northern to northeastern part of the island. According to Nakamura *et al.* (1999), the Maja Formation and Aka Formation consist mainly of sandstone and siltstone. Nakamura *et al.* (1999) also reported 7.8-7.2 Ma for the Maja Formation and 3.2-3.1 Ma for the Aka Formation, respectively, on the basis of $^{87}Sr/^{86}Sr$ ratios of molluscan fossil specimens from both Formations.

The Uegusukudake Formation conformably overlies the Aka Formation (Nakamura *et al.*, 1999), and most part of the Formation is exposed in northwestern part of Kume-jima

(Fig. 1). This Formation, with an exposed thickness of approximately 300 m, is composed of lavas and pyroclastic rocks with subordinate dikes. Such lavas and dikes can be grouped into four types based on their petrological characteristics: (1) picrite basalt (PB) lava; (2) aphyric, tholeiitic basalt and basaltic andesite (A-TH) lavas; (3) porphyritic, tholeiitic basaltic andesite (P-TH) lavas; and (4) porphyritic, calc-alkaline basaltic andesite and andesite (CA) lavas and dikes, in ascending stratigraphic order. The PB lava (~30 m thick) occurs along the northern coast, and was dated by the K-Ar method at 2.76±0.48 Ma (Ito and Shiraki, 1999). The A-TH lavas overlie the PB lava, and consist of about ten flow units. Most of the A-TH lavas are relatively thin with less than 10 m. K-Ar age of 2.13±0.19 Ma was obtained for the A-TH lava from the middle horizon of the Formation (Kitagawa and Shinjo, 2001). The P-TH lavas consist of a few thin (5-10 m) flow units. The CA type is composed of lava flows (10-50 m thickness) and dikes. The dikes of the CA type intrude into the PB lava. K-Ar age of 2.24±0.10 Ma was obtained for the CA lava (Miki, 1995).

The Quaternary Ryukyu Group (the Kitahara Formation) unconformably overlies the Uegusukudake Formation. The Kitahara Formation is mainly composed of loose limestone (Nakagawa and Murakami, 1975).

3. Analytical methods

Some constituent minerals, mainly phenocrysts, were analyzed by two electron probe microanalyzers, a JEOL JCXA-733 at the Ocean Research Institute of the University of Tokyo and a Shimazu EPMA V-6 at the Center of Instrumental Analysis of Yamaguchi University. Operating conditions were 15 kV accelerating voltage and 12 nA (JCXA-733) and 15 nA (EPMA V-6) sample current with a 10 sec counting time with the correction procedure of Bence and Albee (1968).

Whole-rock major element compositions were determined by a X-ray fluorescence (XRF) spectrometry (a Rigaku RIX3000 system), at the Center of Instrumental Analysis, Yamaguchi University, following the procedure of Nagao *et al.* (1997). Trace element concentrations were measured by a inductively-coupled plasma mass spectrometry (ICP-MS) using a Yokogawa Analytical Systems HP4500 at the University of the Ryukyus. Details of the analytical procedure are provided in Shinjo *et al.* (2000). $^{87}Sr/^{86}Sr$ and $^{143}Nd/^{144}Nd$ analyses were performed on unleached whole-rock powders, using a Finnigan MAT262 mass spectrometer at the University of the Ryukyus. During this study, the Sr standard (NBS987) gave a mean $^{87}Sr/^{86}Sr$ of 0.710220 ± 15 (n=3), and the Nd standard (La Jolla) gave a mean $^{143}Nd/^{144}Nd$ of 0.511840 ± 9 (n=4).

Table 1. Representative modal compositions of the samples

Type	Sample	Phenocryst & microphenocryst (vol. %)				
		Pl	Ol	Cpx	Opx	Opq
CA	Dz 7	22.7	–	3.6	2.1	1.0
	Dz 3	21.1	–	1.1	1.7	0.1
	100110	17.9	–	3.4	3.2	1.1
	82001	22.4	–	1.5	2.1	1.3
P-TH	81802	32.0	1.0	–	0.1	trace
	93009	19.1	–	–	0.1	–
A-TH	81105	0.1	trace	trace	–	trace
	92912	1.2	–	–	–	0.2
	92907	1.7	–	0.1	0.7	–
PB	DB 9	0.1	19.8	12.8	–	trace
	DB 1	2.4	11.7	10.6	–	trace
	KB*	–	18.1	9.1	–	–

* Shinjo (1999); Pl, plagioclase; Ol, olivine; Cpx, clinopyroxene; Opx; orthopyrpxene; Opq; opaque mineral.

4. Petrography

The phenocryst assemblages and modal compositions of the representative samples from the Uegusukudake Formation are listed in Table 1. The petrographic and mineralogical features for each type of rocks from the Uegusukudake Formation are described below.

Picrite basalt (PB)

The PB samples are porphyritic with 25-33 vol.% of phenocrysts, and contain olivine, clinopyroxene, plagioclase, and opaque oxide. Olivine phenocrysts, up to 3 mm in diameter, constitute 5-20 vol.%. They occur as both euhedral and anhedral crystals. Anhedral phenocrysts are partially embayed. Regardless of the shapes of crystals, the Fo ($100xMg/(Mg+Fe_{total})$) of olivine phenocrysts at the cores ranges from Fo_{92} to Fo_{85}, and decrease to rims ($<Fo_{80}$). The NiO content at the cores are up to 0.4 wt.%. Chromite spinels ($Cr/(Cr+Al)=0.81-0.63$) are common as inclusions in olivine phenocrysts and occasionally in clinopyroxene phenocrysts. Clinopyroxene phenocrysts (up to 4 mm) occur as euhedral and subhedral short columnar crystals. The cores of clinopyroxene phenocrysts span a compositional range from diopside through endiopside to augite. The values of Mg# ($100xMg/(Mg+Fe_{total})$) at the cores vary from 87 to 78. The Cr_2O_3 contents at the cores are up to 0.85 wt.%. Plagioclase (<2.4 vol.%) occurs as phenocryst and

microphenocryst (up to 2 mm) with euhedral to subhedral outlines. The groundmass shows intersertal texture and consists of plagioclase, clinopyroxene, opaque oxides and subordinate glass.

Aphyric, tholeiitic basalt and basaltic andesite (A-TH)

All products of this type are aphyric with total phenocryst contents less than 7 vol.%. The phenocrysts and microphenocrysts consist of plagioclase and subordinate amount of olivine, orthopyroxene, clinopyroxene, and opaque oxides. Plagioclase phenocrysts (<7 vol.%) are euhedral to subhedral, and are up to 3 mm. The phenocryst cores have a range of An mol.% (100xCa/(Ca+Na+K)) from 83 to 74, and crystals show normal zoning. Olivine (<0.5 vol.%) occurs as microphenocrysts (<0.5 mm), and constitutes up to 0.5 vol.%. They are completely replaced by iddingsite. Orthopyroxene (<0.7 vol.%) and clinopyroxene (<0.5 vol.%) occur as phenocryts and microphenocrysts (<1 mm), and show euhedral and subhedral prismatic shapes. The groundmass shows intersertal texture, and consists of plagioclase, clinopyroxene, opaque oxide, and subordinate amount of glass and silica minerals.

Porphyritic, tholeiitic basaltic andesite (P-TH)

The P-TH lavas are porphyritic, containing 15 to 33 vol.% phenocrysts and microphenocrysts of plagioclase, rare olivine, orthopyroxene, clinopyroxene, and opaque oxides. Plagioclase (<5 mm) is by far the most abundant phase, amounting up to 78-99 % of the assemblage in all the samples. Plagioclase phenocrysts commonly show normal zoning, but some are reversely zoned. The compositional range of the cores of the normally-zoned phenocrysts is from An_{87} to An_{74}, whereas reversely-zoned phenocrysts have cores with An mol.% <65. The An mol.% of the rims ranges from 76 to 59. Orthopyroxene (<0.2 vol.%) and clinopyroxene (<0.6 vol.%) rarely occur as euhedral and subhedral microphenocrysts, and are up to 1 mm. Olivine microphenocrysts (<3 vol. %) are completely altered to iddingsite. The groundmass is composed of plagioclase, clinopyroxene, opaque oxide, glass, and silica minerals.

Porphyritic, calc-alkline basaltic andesite and andesite (CA)

The CA samples contain 12 to 40 vol.% phenocrysts and microphenocrysts. The phenocryst assemblage is plagioclase + orthopyroxene + clinopyroxene + opaque minerals ± olivine. Plagioclase phenocrysts (<3 mm) constitute 9-34 vol.% of the samples. The composition of the plagioclase cores ranges from An_{90} to An_{50}, regardless of the whole-rock compositions. The phenocrysts having cores with An mol.% of >70 commonly show normal zoning, whereas the phenocrysts having more sodic cores (An <70) show reverse zoning. Some of these reversely-zoned phenocrysts have sieve-textured dusty zone in their margins. Orthopyroxene phenocrysts and microphenocrysts (0.6-3.8 vol.%), up to 2 mm,

have cores with Mg# rainging from 77 to 58. Normally-zoned phenocrysts generally have cores with Mg# of >65, whereas reversely-zoned phenocrysts are Mg# of <65. Clinopyroxene phenocrysts, up to 2 mm in length, constitute 0.2 to 3.8 vol.%, and occur as euhedral~subhedral short columnar crystals. They are augite and have large homogeneous cores ($Wo_{38-43}En_{45-38}Fs_{14-22}$). Olivine phenocrysts (<1.5 mm) are rarely present in the CA samples and most of them are replaced by iddingsite. The groundmass has intersertal to hyalo-ophitic texture, consisting of plagioclase, clinopyroxene, orthopyroxene, opaque oxide, glass, and silica minerals. The groundmass in some CA samples is heterogeneous in terms of textures with various scale.

5. Whole-rock geochemical compositions

Whole-rock major and trace elements and isotopic compositions for representative samples from the Uegusukudake Formation are listed in Table 2. Analyses of the sample KB are from Shinjo (1999).

Major and trace element variations

In SiO_2-K_2O diagram (Fig. 2a), all samples of the Uegusukudake Formation fall in the range of the medium-K series (Le Maitre *et al.*, 1989). Figure 2b is a plot of FeO* (total Fe as FeO)/MgO versus SiO_2, in which the A-TH and P-TH samples show trends having gentler slopes than the boundary line between tholeiitic and calc-alkaline series (Miyashiro, 1974), and can be classified as tholeiitic rock series. On the other hand, the CA samples have a trend having almost the same slope as that of the boundary line, and are classified as calc-alkaline rock series.

Selected major and trace element variations, utilizing FeO*/MgO ratio as a differentiation index, are shown in Figure 3. TiO_2 and FeO* contents of the individual types of samples show linear trends against the FeO*/MgO, and the difference among the variation trends for each type can be recognized. In Na_2O, K_2O, Rb and Ba versus FeO*/MgO diagrams, plots are somewhat scattered for individual types. These features are presumably as a result of weathering because these elements (Na, K, Rb and Ba) are relatively mobile under weathering processes (e.g. Chesworth *et al.*, 1981; Eggleton *et al.*, 1987; Marsh, 1991; Nesbitt and Wilson, 1992).

All rare-earth element (REE) data normalized to chondrite abundances (Boynton, 1984) are plotted in Figure 4. All samples from the Uegusukudake Formation show light REE (LREE)-enriched patterns. Some samples have negative Ce anomaly, which is a typical feature of incipient weathering of basic volcanic rocks (Marsh, 1991; Price *et al.*, 1991; Nesbitt and Wilson, 1992). In the following discussions, therefore, the samples with negative Ce anomaly are eliminated. Although the REE patterns of all types are similar, slight differences in element ratios (La/Sm) are observed (Fig. 5). Excluding the PB

Table 2. Major, trace and Sr-Nd isotopic compositions of volcanic rocks from the Uegusukudake Formation

Type	PB		A-TH							
	KB*	50201	92901L1	92901L2	92910L3	92905-1	92905-2	92907	92912	81105
(wt. %)										
SiO_2	50.89	49.76	50.80	50.87	48.95	49.61	49.83	50.42	51.43	52.71
TiO_2	0.84	0.86	1.86	2.03	2.04	1.81	2.00	1.61	1.96	1.68
Al_2O_3	14.12	15.62	19.01	18.80	19.08	19.12	17.78	19.25	17.03	19.43
Fe_2O_3 (total)	9.91	8.77	9.84	10.44	11.93	10.95	12.43	9.61	12.65	9.86
MnO	0.15	0.15	0.21	0.31	0.25	0.19	0.20	0.16	0.19	0.16
MgO	11.06	8.93	3.31	3.31	3.72	3.57	3.60	4.66	2.98	3.38
CaO	10.26	10.39	8.42	7.24	8.38	8.33	7.83	9.04	6.76	6.77
Na_2O	2.11	2.34	3.29	3.38	3.04	3.13	2.96	2.62	3.05	3.51
K_2O	0.71	0.76	0.75	0.82	0.39	0.61	0.84	0.64	1.08	1.21
P_2O_5	0.11	0.08	0.17	0.19	0.12	0.15	0.23	0.10	0.14	0.17
Total	100.16	97.65	97.66	97.39	97.88	97.46	97.70	98.10	97.27	98.86
(ppm)										
Sc	36.6		33.4	36.3	35.0	32.6	33.7	37.8	35.0	
V	255		328	296	315	308	318	388	404	
Cr	479		19	3	11	24	25	50	6	
Co	47		30	29	32	30	31	34	32	
Ni	171		12	5	12	16	16	20	13	
Rb	13.2		23.1	17.5	8.1	17.1	17.5	22.6	39.7	
Sr	383		208	203	205	196	202	218	187	
Y	19.4		44.5	44.6	34.9	36.6	37.6	29.8	50.7	
Zr	72		149	178	195	138	141	107	141	
Nb	2.1		4.7	6.0	6.5	4.4	4.5	3.4	4.3	
Cs	0.32		1.99	1.18	0.80	1.34	1.36	1.64	2.99	
Ba	124		177	245	148	127	128	158	208	
Hf	1.97		3.94	4.73	4.94	3.58	3.58	2.84	3.75	
Ta	0.15		0.24	0.34	0.34	0.21	0.21	0.12	0.24	
Pb	4.49		8.72	10.61	9.51	7.68	7.66	8.33	11.93	
Th	2.37		2.46	3.22	2.90	2.34	2.33	2.76	3.69	
U	0.64		0.74	0.89	0.36	0.49	0.48	0.70	1.01	
La	8.10		13.00	14.70	9.50	11.40	11.50	10.30	17.20	
Ce	18.50		29.99	33.05	23.58	26.10	26.21	22.45	32.41	
Pr	2.52		4.12	4.69	3.10	3.75	3.75	2.99	5.25	
Nd	11.50		19.65	22.01	14.80	17.66	17.85	13.61	25.00	
Sm	3.02		5.61	6.13	4.31	4.92	5.01	3.83	7.11	
Eu	1.00		1.77	2.00	1.85	1.62	1.66	1.25	2.00	
Gd	3.19		6.89	7.33	5.26	5.97	6.10	4.67	8.68	
Tb	0.53		1.24	1.32	0.99	1.05	1.07	0.82	1.53	
Dy	3.24		7.81	8.12	6.16	6.61	6.59	5.16	9.29	
Ho	0.69		1.68	1.72	1.35	1.39	1.41	1.12	1.96	
Er	2.00		4.93	5.06	4.09	4.01	4.08	3.30	5.70	
Tm	0.30		0.77	0.78	0.64	0.61	0.62	0.51	0.87	
Yb	1.89		4.94	4.98	4.22	4.00	4.00	3.23	5.51	
Lu	0.29		0.76	0.76	0.65	0.60	0.61	0.50	0.84	
$^{87}Sr/^{86}Sr$	0.703465 ± 31				0.704573 ± 14			0.704795 ± 19	0.704661 ± 14	
$^{143}Nd/^{144}Nd$	0.512903 ± 17							0.512753 ± 17	0.512767 ± 8	

* Data from Shinjo (1999).

Table 2. Continued

Type	A-TH	P-TH				CA			
	81107	92909	93009	81801	81802	GML	82001	50102	81508
(wt, %)									
SiO_2	52.79	51.53	51.18	52.92	52.14	56.55	56.64	57.64	55.32
TiO_2	1.81	1.28	1.23	1.14	0.98	0.88	0.82	0.88	0.79
Al_2O_3	17.84	19.44	20.35	19.70	20.86	19.08	20.26	17.97	19.42
Fe_2O_3 (total)	9.92	9.96	9.73	9.58	8.34	7.73	6.53	8.10	8.20
MnO	0.17	0.16	0.14	0.15	0.13	0.12	0.12	0.13	0.13
MgO	3.72	3.53	3.57	2.96	2.59	2.89	2.06	2.82	3.28
CaO	7.78	7.95	8.35	7.29	7.95	6.44	5.93	5.79	6.48
Na_2O	3.45	3.05	2.65	3.09	3.01	3.31	3.52	3.26	3.11
K_2O	0.96	0.79	0.95	1.15	0.96	1.28	1.63	1.26	1.12
P_2O_5	0.13	0.09	0.14	0.21	0.15	0.09	0.14	0.09	0.11
Total	98.56	97.79	98.27	98.17	97.12	98.37	97.65	97.94	97.95
(ppm)									
Sc		29.6	31.0	27.1	25.1	22.6	20.4		22.2
V		340	291	258	260	187	121		194
Cr		34	27	8	7	13	2		11
Co		34	27	29	25	20	15		24
Ni		18	21	7	8	6	2		10
Rb		25.6	34.7	35.8	34.4	51.0	46.1		38.7
Sr		231	227	297	322	167	262		225
Y		23.2	29.0	35.3	48.4	23.8	34.2		52.5
Zr		80	108	108	87	108	113		93
Nb		2.2	3.3	3.6	2.8	3.2	4.0		3.4
Cs		1.41	2.79	4.11	6.80	2.09	3.83		2.24
Ba		143	215	260	222	152	301		248
Hf		2.21	2.93	2.83	2.27	2.80	2.96		2.52
Ta		0.05	0.13	0.12	0.09	0.19	0.19		0.16
Pb		8.27	10.14	10.55	6.97	9.59	12.14		9.70
Th		2.35	2.83	2.65	2.16	3.64	3.58		3.12
U		0.71	0.84	0.80	0.64	1.30	1.05		0.95
La		8.34	14.04	15.47	14.94	10.36	16.88		24.88
Ce		18.90	29.38	35.29	28.72	22.98	34.34		26.77
Pr		2.44	4.16	4.60	4.83	2.94	4.73		7.06
Nd		11.1	18.42	20.74	22.91	12.86	21.14		31.94
Sm		3.04	4.74	5.27	6.40	3.36	5.24		7.66
Eu		1.10	1.41	1.55	1.98	1.07	1.59		2.51
Gd		3.63	5.18	6.09	7.89	3.79	5.89		9.11
Tb		0.66	0.89	1.01	1.29	0.67	0.98		1.49
Dy		4.04	5.36	6.21	7.80	4.22	5.77		8.74
Ho		0.89	1.12	1.32	1.64	0.89	1.23		1.82
Er		2.65	3.26	3.85	4.63	2.64	3.59		5.22
Tm		0.41	0.51	0.58	0.69	0.41	0.55		0.77
Yb		2.63	3.23	3.66	4.25	2.67	3.46		4.80
Lu		0.41	0.50	0.56	0.66	0.41	0.55		0.74
$^{87}Sr/^{86}Sr$		0.704689 ± 14	0.704690 ± 16	0.704579 ± 16	0.704541 ± 16		0.704904 ± 15		
$^{143}Nd/^{144}Nd$		0.512721 ± 7	0.512753 ± 9	0.512726 ± 8	0.512725 ± 8		0.512695 ± 8		

Table 2. Continued

Type	100110	Dz3	DZ4b	92801	Dz7
(wt. %)					
SiO_2	53.79	52.90	54.57	60.62	57.86
TiO_2	0.93	0.73	0.69	0.80	0.71
Al_2O_3	19.63	20.88	21.61	17.82	19.99
Fe_2O_3 (total)	8.55	7.41	6.57	5.88	6.25
MnO	0.13	0.11	0.11	0.08	0.11
MgO	3.50	4.07	2.24	1.87	2.31
CaO	7.11	8.58	7.93	4.47	6.53
Na_2O	3.02	2.31	2.88	3.80	3.16
K_2O	1.04	1.06	0.98	1.71	1.43
P_2O_5	0.12	0.07	0.09	0.14	0.09
Total	97.81	98.12	97.68	97.19	98.44
(ppm)					
Sc	27.1	28.7	20.7	19.3	24.7
V	232	232	149	78	150
Cr	8	17	5	12	12
Co	23	26	16	13	17
Ni	9	18	8	6	9
Rb	32.6	35.8	28.9	64.4	56.4
Sr	244	194	175	191	139
Y	24.2	19.1	23.0	31.1	24.5
Zr	92	76	86	118	104
Nb	3.0	2.2	2.5	4.7	3.2
Cs	1.18	2.90	2.55	2.73	4.77
Ba	205	122	123	289	176
Hf	2.49	2.03	2.33	3.13	2.73
Ta	0.08	0.10	0.11	0.29	0.19
Pb	11.44	8.38	8.98	13.92	11.22
Th	2.33	2.89	2.75	4.78	4.31
U	0.73	1.14	0.95	1.48	1.70
La	11.99	8.49	8.83	15.67	11.38
Ce	25.36	18.83	20.07	35.00	25.59
Pr	3.35	2.30	2.52	4.25	3.08
Nd	15.02	9.91	11.27	18.62	13.14
Sm	3.71	2.63	2.96	4.62	3.35
Eu	1.18	0.80	0.92	1.25	0.92
Gd	4.12	3.04	3.57	5.17	3.88
Tb	0.70	0.53	0.63	0.87	0.66
Dy	4.18	3.28	3.99	5.44	4.20
Ho	0.90	0.71	0.85	1.15	0.90
Er	2.65	2.08	2.51	3.32	2.65
Tm	0.41	0.32	0.39	0.51	0.41
Yb	2.64	2.09	2.58	3.32	2.73
Lu	0.41	0.32	0.41	0.51	0.42
$^{87}Sr/^{86}Sr$	0.704788 ± 23	0.704952 ± 16			0.705369 ± 16
$^{143}Nd/^{144}Nd$	0.512719 ± 7	0.512712 ± 8			0.512697 ± 8

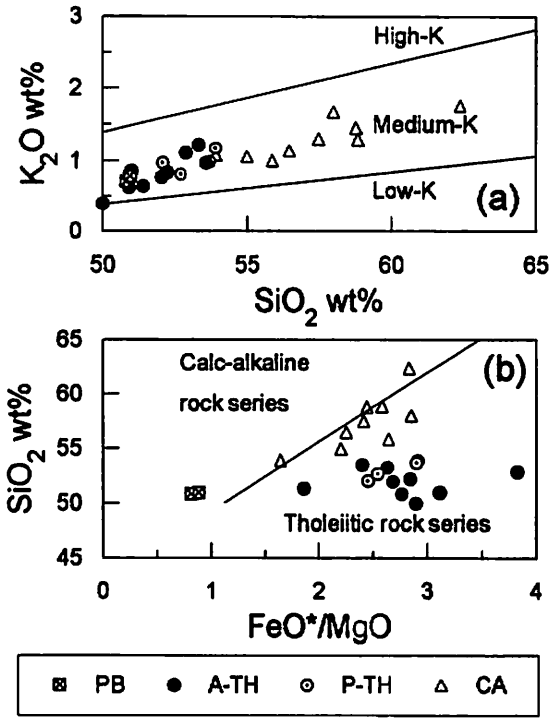

Figure 2. (a) SiO_2 - K_2O diagram for the volcanic rocks from the Uegusukudake Formation. High-, medium- and low-K discriminant lines are from Le Maitre et al. (1989). (b) FeO*/MgO - SiO_2 diagram. Boundary line is from Miyashiro (1974).

sample, these ratios tend to increase from the A-TH through P-TH to CA, and are relatively homogeneous for each type.

Figure 6 shows the N-MORB normalized incompatible trace element abundance diagrams. Despite of the different degree of weathering, these samples have relatively coherent patterns. All the Uegusukudake volcanic rocks are enriched in large ion lithophile elements (LILE), such as Cs, Rb, and Ba, relative to high field strength elements (HFSE), such as Zr, Hf, and Nb. These geochemical characteristics are typical of island-arc volcanic rocks (e.g., Perfit *et al.*, 1980; Hawkesworth *et al.*, 1993). Excluding the PB sample, the three types of volcanic rocks show similar normalized patterns. However, Nb-Ta troughs in patterns of the A-TH samples are less pronounced than those of the P-TH and CA samples. The normalized pattern of the PB sample is slightly different from those of the other types of rocks. The PB sample has lower abundance of Cs relative to the other LILE (Rb, Ba and K) (thus lower Cs/K) in comparison with the other types (Fig. 7).

Sr-Nd isotopic compositions

Sr and Nd isotopic ratios of the representative samples are plotted against the FeO*/MgO in Figure 8. The PB sample has a different isotopic composition, characterized

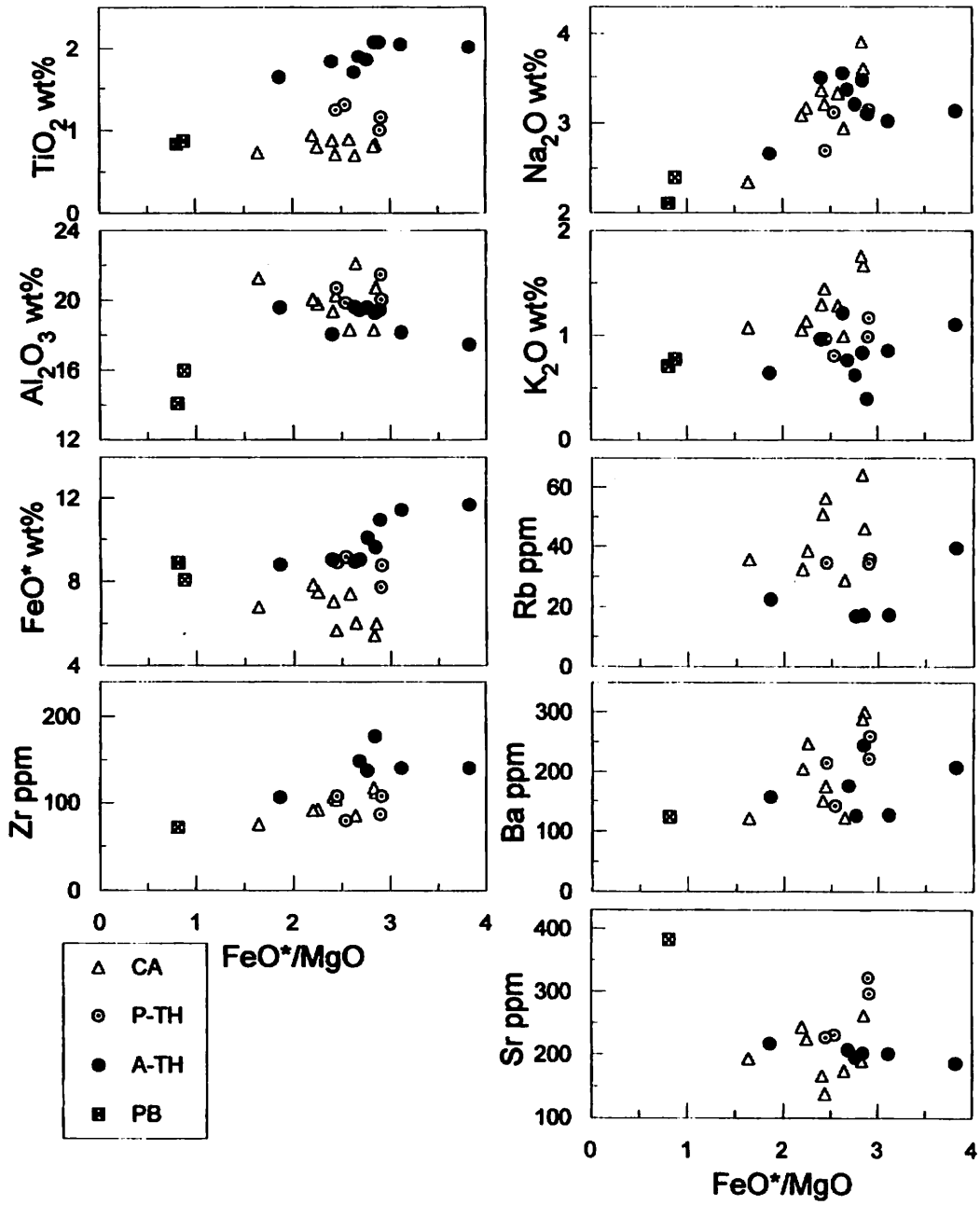

Figure 3. Variation diagrams for selected major and trace elements against FeO*/MgO.

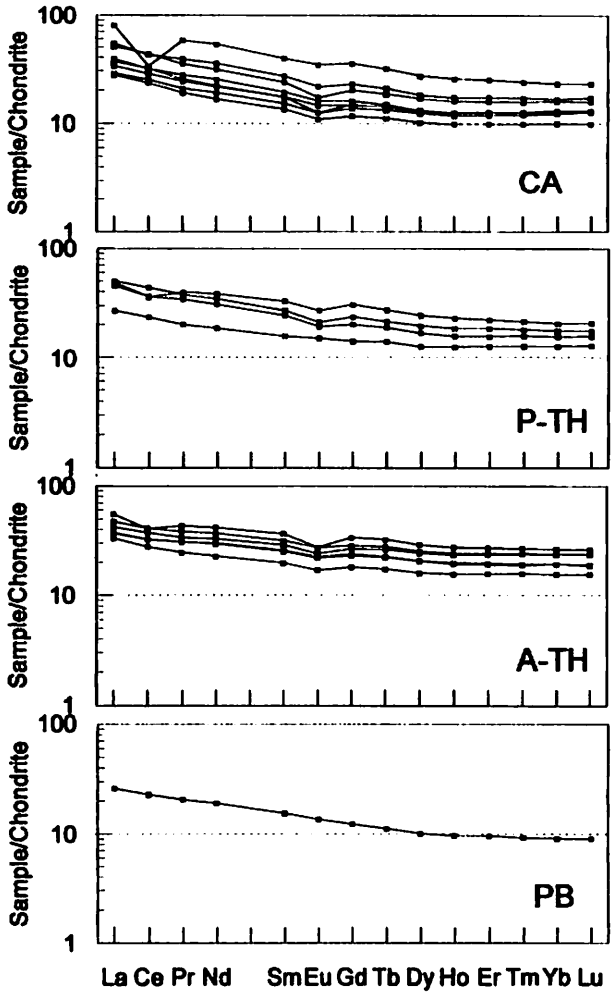

Figure 4. Chondrite-normalized REE patterns for the samples. The normalization values are from Boynton (1984).

by significantly low $^{87}Sr/^{86}Sr$ (0.70347) and high $^{143}Nd/^{144}Nd$ (0.51290), compared with the other Uegusukudake volcanic rocks (A-TH, P-TH and CA). The A-TH, P-TH and CA types are relatively similar in Sr and Nd isotopic ratios, but slight differences are observed among the types (Fig. 8). $^{87}Sr/^{86}Sr$ of the CA samples (0.70479-0.70537) are somewhat higher than that of the A-TH samples (0.70457-0.70480) and the P-TH samples (0.70454-0.70469). Nd isotopic ratios of the A-TH, P-TH and CA samples are in the range between 0.512695 and 0.512839. Excluding the PB sample, the A-TH samples have the highest $^{143}Nd/^{144}Nd$ (0.512753-0.512839) and CA have the lowest $^{143}Nd/^{144}Nd$ (0.512695-0.512719).

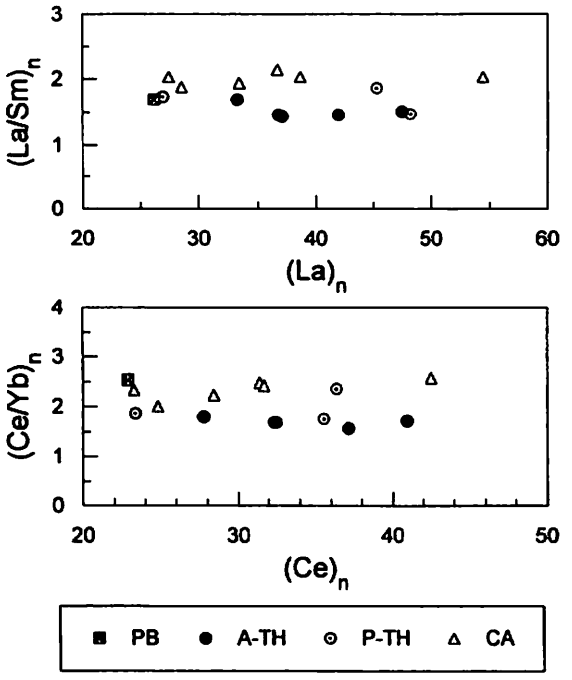

Figure 5. Chondrite-normalized $(La)_n$ - $(La/Sm)_n$ variation diagram.

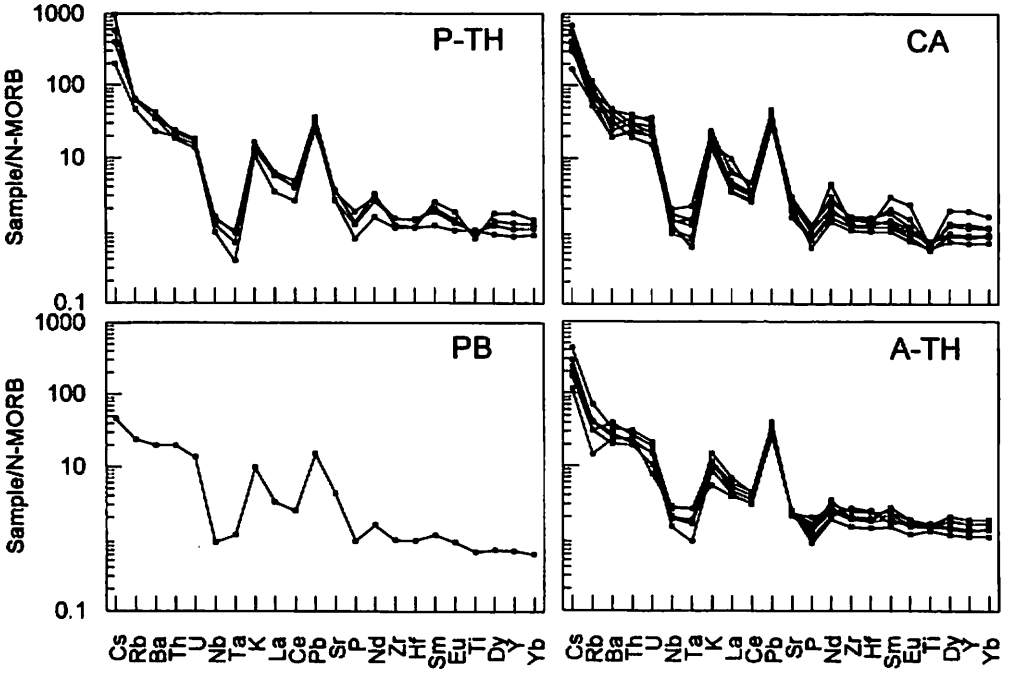

Figure 6. N-MORB normalized trace element patterns for the samples. The N-MORB values are from Sun and McDonough (1989).

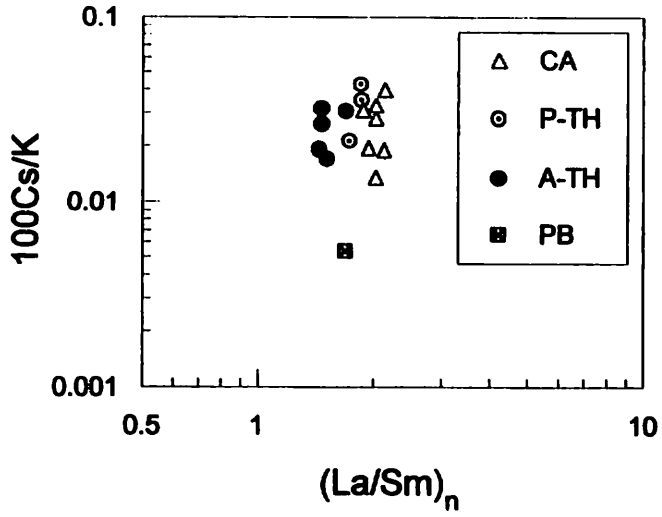

Figure 7. 100Cs/K ratios of the Uegusukudake volcanic rocks plotted against $(La/Sm)_n$.

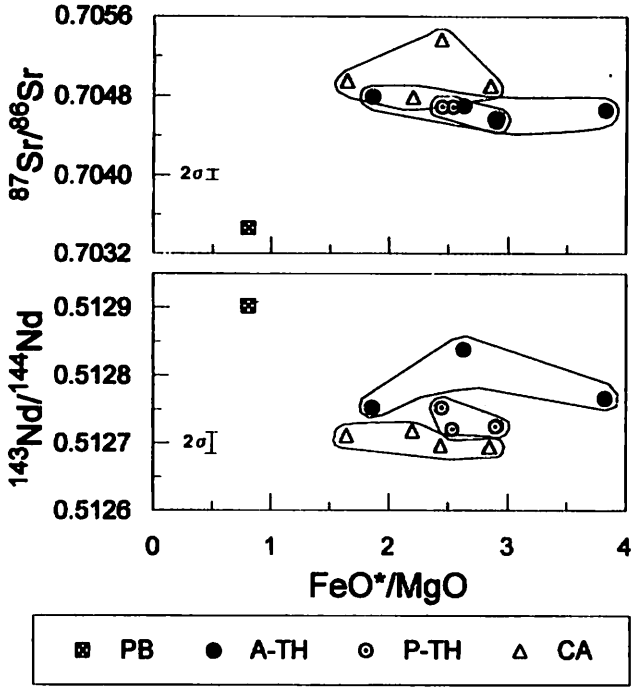

Figure 8. Sr and Nd istopic compositions of the samples plotted against FeO*/MgO.

6. Discussion

Source characteristics

The compositional varieties of erupted magmas are attributed to several magmatic processes. Magmatic processes in closed system such as partial melting, melt migration, and magmatic defferentiation are generally thought to have little effect on diversing isotopic compositions of magmas. The concentration ratios of two trace elements having similar bulk partition coefficients are also not affected by such processes (Minster and Allègre, 1978). On the other hand, trace and isotopic compositions of magmas are sensitive to the processes in open system such as mixing of magmas having distinct trace and isotopic compositions, and crustal assimilation (e.g. DePaolo, 1981). Thus, the trace element abundances and Sr and Nd isotopic ratios of the samples are useful for evaluating magmatic processes.

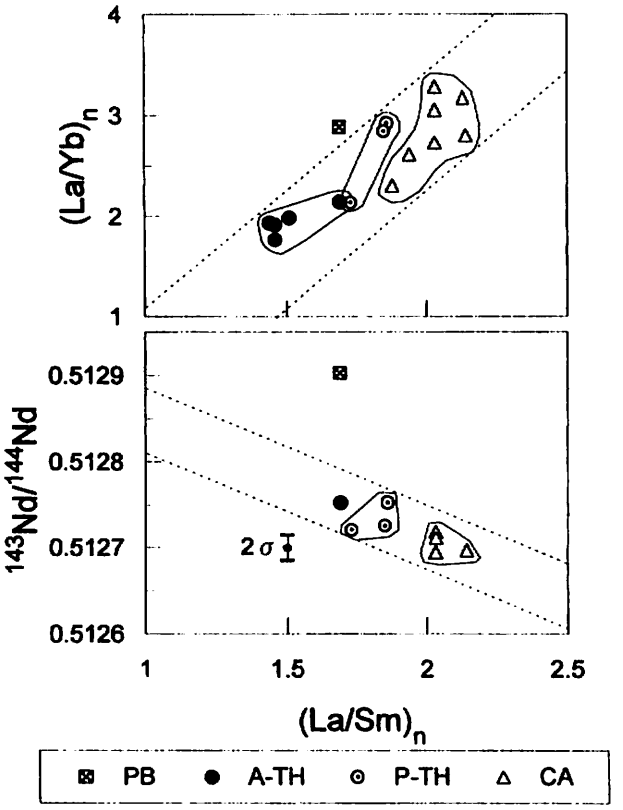

Figure 9. Plot of (La/Yb)n and $^{143}Nd/^{144}Nd$ against $(La/Sm)_n$. In $(La/Sm)_n$ - $^{143}Nd/^{144}Nd$ diagram, only one sample of the A-TH type is plotted, because the other samples of this type have no REE data or showing Ce anomaly in Figure 4.

$(La/Yb)_n$ and $^{143}Nd/^{144}Nd$ plotted against $(La/Sm)_n$ are shown in Figure 9. The A-TH, P-TH and CA samples form linear trends, indicating that they have simple co-genetic relations. The PB sample, however, has a composition that significantly deviates from the linear trend in $^{143}Nd/^{144}Nd$-$(La/Sm)_n$ diagram. The PB sample is also distinct from the other three types of rocks in Figure 7, characterized by low Cs/K ratio. These deviations cannot be explained by magmatic processes such as fractional crystallization of a common parental magma, and different degree of partial melting of a single source mantle. Although the difference of isotopic compositions may favor magma mixing or crustal assimilation, these also fail to account for the deviations. This is because the PB sample have intermediate $(La/Sm)_n$ between A-TH and CA samples, on the other hand, the PB sample has the highest $^{143}Nd/^{144}Nd$ ratio in all rock types (Fig. 9). This indicates that the simple two-component mixing of the PB magma and another magma or crustal material cannot produce the variations of the A-TH, P-TH, and CA rocks. From these, the deviations of the PB sample in Figures 7, 8, and 9 cannot have been due to any crustal magmatic proceses, and therefore they are considered to have resulted from the heterogeneity of the source mantle. This implies the presence of at least two components in the source mantle beneath Kume-jima: isotopically depleted source with low Cs/K ratio, and isotopically enriched source with high Cs/K ratio.

Magmatic processes in A-TH, P-TH, and CA magmas

As shown in the previous section, the geochemical data of volcanic rocks suggest that the PB and the other types of rocks were inherited from distinct source mantles. Although the A-TH, P-TH, and CA magmas are considered to have been derived from the common source material, as suggested from similar trace element patterns (Fig. 6), slight differences in Sr and Nd isotopic and some trace element ratios (Figs. 5, 8, and 9) are observed. In the following, we consider the possible explanations for differences in isotopic and trace element ratios among these three types of rocks, and then discuss the magmatic processes responsible for forming compositional variations of each type of magmas.

Origin of heterogeneity among the A-TH, P-TH, and CA magmas

In Figure 5, the A-TH, P-TH, and CA samples show linear trends with flat or very gentle slopes, and each three type falls on the slightly different horizontal trends. Fractionation or accumulation of the observed phenocryst assemblages in the Uegusukudake volcanic rocks cannot account for the differences of these element ratios (Minster and Allègre, 1978) as well as Sr and Nd isotopic ratios (Fig. 8). This suggests that three types of magmas cannot be derived from a common parental magma solely by crystal fractionation or accumulation, and that each type of magmas evolved either in distinct closed systems (i.e. distinct magma chambers) or from different parts in a single but heterogeneous system (i.e. different parts in a single magma chamber).

In Figure 9, the La/Sm, La/Yb and Nd isotopic ratios successively change from the A-TH through P-TH to CA samples. The simplest possibility for the linear trends in Figure 9 is two component mixing. The gradual changes in trace and isotopic ratios can be attributed to the mixing of depleted (low La/Sm, La/Yb, and $^{143}Nd/^{144}Nd$) and enriched (high La/Sm, La/Yb, and $^{143}Nd/^{144}Nd$) components. The A-TH samples are aphyric and have no petrological evidence for magma mixing, and therefore would have been a depleted end component. However, the P-TH magma cannot have been a mixing product between the A-TH and CA magmas, because most P-TH samples don't have obvious evidence for magma mixing, and the mineralogical features of the P-TH and CA rocks are quite different. The magma mixing was, therefore, not responsible for forming geochemical variations among the A-TH, P-TH, and CA rocks. From this, it is plausible to consider that parental magmas of each type ingested a crustal material in slightly different degrees, and then they evolved as a closed system. The most compelling evidence for this interaction is the systematic change in Nd isotopic ratios; $^{143}Nd/^{144}Nd$ decreases with the order from the A-TH through P-TH to CA samples (Fig. 9). Although the trace element composition of the crustal material beneath Kume-jima cannot be obtained directly, the upper crustal material is generally thought to have high LREE/medium REE (e.g. La/Sm) and LREE/heavy REE (e.g. La/Yb) ratios (Taylor and McLennon, 1995; Wedepohl, 1995; Gao *et al.*, 1998). Although Sr and Nd isotopic ratios of the crustal material are also unknown, the upper crustal material beneath the middle Okinawa Trough, just behind the central Ryukyu Arc is considered to have high $^{87}Sr/^{86}Sr$ (~0.7103) and low $^{143}Nd/^{144}Nd$ (~0.5123) ratios (Shinjo and Kato, 2000). This is because the geological character beneath the middle Okinawa Trough is similar to that of the Inner Zone of southwest Japan (Kizaki, 1986), which is characterized by widespread exposure of late Cretaceous to early Paleogene acidic plutonic rocks having high $^{87}Sr/^{86}Sr$ and low $^{143}Nd/^{144}Nd$ ratios (Terakado and Nakamura, 1984). Kume-jima is located in the Inner Zone of the Ryukyu Arc, and stands on the eastern edge of the Okinawa Trough. Crustal material under Kume-jima would therefore be similar to that of the middle Okinawa Trough. Thus, the crustal material could be a possible candidate for the assimilant, and the A-TH, P-TH, and CA rocks can be ascribed to change in the degree of crustal assimilation. In this case, the degree of assimilation increases from the A-TH through P-TH to CA rocks.

Origin of heterogeneity within the A-TH, P-TH, and CA magmas

Contrary to the differences among the individual types of rocks, the compositional variations for each type were produced by either crystal fractionation or accumulation in closed systems. Figure 10 shows the relation between the whole-rock Al_2O_3 contents and modal abundances of plagioclase phenocrysts, in which positive correlations between whole-rock Al_2O_3 content and modal abundance of plagioclase are observed in the P-TH rocks. This suggests that plagioclase phenocrysts selectively accumulated in the P-TH magmas. In REE

patterns of the P-TH samples (Fig. 4), there is no sample exhibiting marked positive Eu anomalies. However, the absence of positive Eu anomalies does not necessarily indicate that plagioclase has not accumulated, since the groundmass of the arc basaltic and andesitic rocks have significant negative Eu anomalies in general, and there can be a case that plagioclase accumulation only diminish negative Eu anomalies (Crawford *et al.*, 1987). MgO/Al_2O_3 versus Sr/Zr variation diagram is given in Figure 11. Fractionation of phenocryst phases including plagioclase and mafic minerals from basaltic and andesitic

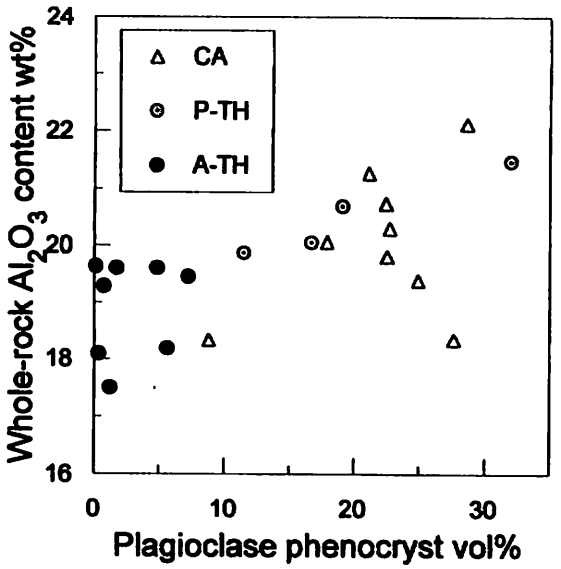

Figure 10. Modal abundances of plagioclase phenocysts vs. whole-rock Al_2O_3 contents of the samples.

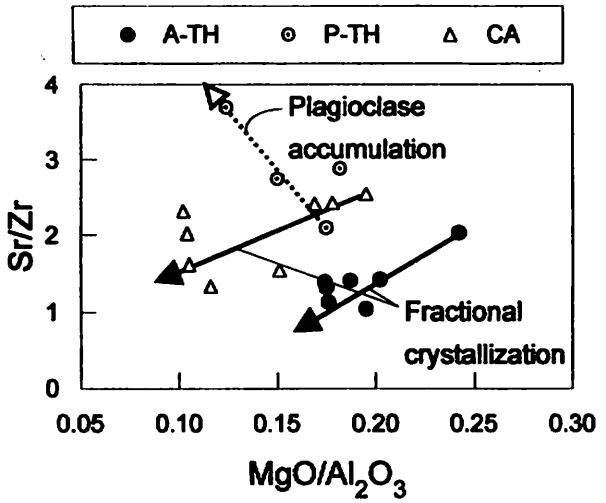

Figure 11. MgO/Al_2O_3 vs. Sr/Zr diagram.

magmas would decrease both Sr/Zr and MgO/Al_2O_3. On the other hand, the accumulation of plagioclase increases Sr/Zr, and decreases MgO/Al_2O_3 in whole-rock compositions, because plagioclase has high Sr/Zr and low MgO/Al_2O_3. The P-TH samples show the trend of increasing Sr/Zr with decreasing MgO/Al_2O_3. This trend supports that plagioclase accumulation plays major role on the formation of the P-TH magma. In contrast, the A-TH and CA samples exhibit the trends decreasing both Sr/Zr and MgO/Al_2O_3, which is consistent with crystal fractionation. Slight scatter of the CA data would be caused by preferential retention of plagioclase in the CA magma due to their low density (Marsh, 1988; Brophy, 1989).

The CA samples have various evidences of magma mixing and mingling, including heterogeneous groundmass and disequilibrium textures in phenocrysts (reverse zoning of some plagioclase and orthopyroxene). Relative coherent isotopic and trace element ratios (La/Sm) within the CA rocks suggest that magma mixing took place in a geochemically homogeneous closed-system magma body. Thus, the internal hybridization in a single magma reservoir is the most plausible model for the interpretation of the petrographical and geochemical characteristics of the CA samples.

7. Conclusions

The conclusions of this study are summarized as follows:

1. The Uegusukudake Formation in Kume-jima is composed of lavas and pyroclastic rocks with subordinate dikes. The volcanic rocks (lavas and dikes) from the Uegusukudake Formation are divided into four types: (1) picrite basalt (PB); (2) aphyric, tholeiitic basalt and basaltic andesite (A-TH); (3) porphyritic, tholeiitic basaltic andesite (P-TH); and (4) porphyritic, calc-alkaline basaltic andesite and andesite (CA).
2. The PB type has significantly different isotopic composition and trace element ratios (Cs/K), implying that the PB magma was derived from the distinct source material from those of the other three types (A-TH, P-TH, and CA). This suggests that at least two types of magmatic sources were present beneath Kume-jima in late Pliocene.
3. A slight difference in isotopic and trace element compositions among the A-TH, P-TH, and CA types can be due to the difference of the contributions of crustal assimilation to geochemically similar magmas. The degree of assimilation increases from the A-TH through P-TH to CA types.
4. The compostional variation of the A-TH type can be explained by a closed-system fractional crystallization from a parental magma. The variation of the CA magma can be explained by internal hybridization within a single magma chamber. For the variation of the P-TH magma, plagioclase accumulation is inferred to have played a dominant role.

Acknowledgements

We thank T. Nagao of Yamaguchi University for XRF and EPMA analyses. We also appreciate T. Ishii, S. Haraguchi, and M. Otsuki of the Ocean Research Institute (ORI) of the University of Tokyo for EPMA analysis (supported by funds from the cooperative program No. 26, 2001, provided by ORI). We acknowledge K. Kobayashi, R. Tanaka T. Kuritani of the Pheasant Memorial Laboratory for Geochemistry and Cosmochemistry at ISEI for constructive discussions. This work was supported by the Grants-in-Aid for Scientific Research (C) from the Ministry of Education, Culture, Sports, Science and Technology, Japan to R.S. (subject No. 13640483). We also thank T. Oomori of the University of the Ryukyus for reading the manuscript.

References

Bence, A.E. and Albee, A.L. (1968) Empirical correction factors for the electron microanalysis of silicates and oxides. *J. Geol.*, 76, 382-403.

Boynton, W.V. (1984) Cosmochemistry of the rare earth elements: meteorite studies. *In* Rare earth element geochemistry (Henderson, P. Ed.). pp. 510, Elsevier, Amsterdam, 63-114.

Brophy, J.G. (1989) Basalt convection and plagioclase retention: a model for the generation of high-alumina arc basalts. *J. Geol.*, 97, 155-172.

Chesworth, W., Dejou, J. and Larroque, P. (1981) The weathering of basalt and relative mobilities of the major elements at Belbex, France. *Geochim. Cosmochim. Acta,* 45, 1235-1243.

Crawford, A.J., Falloon, T.J. and Eggins, S. (1987) The origin of island arc high-alumina basalts. *Contrib. Mineral. Petrol.*, 97, 417-430.

Daishi, M., Hayashi, Y. and Kato, Y. (1987) Radiometric ages of some Cenozoic volcanic rocks from Ryukyu Islands. *J. Japan. Assoc. Mineral. Petr. Econ. Geol.*, 82, 370-381 (in Japanese with English abstract).

DePaolo, D.J. (1981) Trace element and isotopic effects of combined wallrock assimilation and fractional crystallization. *Earth Planet. Sci. Lett.*, 53, 189-202.

Eggleton, R.A., Foudoulis, C. and Varkevisser, D. (1987) Weathering of basalt: changes in rock chemistry and mineralogy. *Clays Clay Mineral.*, 35, 161-169.

Gao, S., Luo, T.-C., Zhang, B.-R., Zhang, H.-F., Han, Y.-w., Zhao, Z.-D. and Hu, Y.-K. (1998) Chemical composition of the continental crust as revealed by studies in East China. *Geochim. Cosmochim. Acta.*, 62, 1959-1975.

Hawkesworth, C.J., Gallagher, K., Hergt, J.M. and McDermott, F. (1993) Mantle and slab contributions in arc magmas. *Ann. Rev. Earth Planet. Sci.*, 21, 175-204.

Ito, J. and Shiraki, K. (1999) Picrite basalts from the Pliocene Uegusukudake Formation

in Kume-jima, Ryukyu Islands. *J. Geol. Soc. Japan*, 105, 810-813 (in Japanese with English abstract).

Kato, Y. (1985) Geology of the Kume-jima Island. *In* Geology of the Ryukyu Arc (Kizaki, K. Ed.). pp. 278, Okinawa Times Co., Naha, 119-123 (in Japanese).

Kitagawa, H. and Shinjo, R. (2001) Whole-rock K-Ar age of a basaltic andesite from the Uegusukudake Formation in Kume-jima, Central Ryukyu Arc. *Japan. Mag. Mineral. Petrol. Sci.*, 30, 237-240 (in Japanese with English abstract).

Kizaki, K. (1986) Geology and tectonics of the Ryukyu Islands. *Tectonophysics*, 125, 193-207.

Le Maitre, R.W., Bateman, P., Dudek, A., Keller, J., Lameyre, P., Le Bas, M.J., Sabine, P.A., Schmid, R., Sorensen, H., Streckeisen, A., Woolley, A.R. and Zanettin, B. (1989) A classification of igneous rocks and glossary of terms: Recommendations of the IUGS subcomission on the systematics of igneous rocks. pp. 204, Blackwell Scientific, Oxford.

Maritime Safety Agency of Japan (1991) The southern seas of Nippon: Bathymetric Chart H-1001, scale 1:2,500,000. Hydrographic and Oceanographic Department, Tokyo.

Marsh, B.D. (1988) Crystal capture, sorting, and retention in convecting magma. *Geol. Soc. Am. Bull.*, 100, 1720-1737.

Marsh, J.S. (1991) REE fractionation and Ce anomalies in weathered Karoo dolerite. *Chem. Geol.*, 90, 189-194.

Miki, M. (1995) Two-phase opening model for the Okinawa Trough inferred from paleomagnetic study of the Ryukyu arc. *J. Geophys. Res.*, 100, 8169-8184.

Minster, J.F. and Allègre, C.J. (1978) Systematic use of trace element in igneous processes part III: inverse problem of batch partial melting in volcanic suites. *Contrib. Mineral. Petrol.*, 68, 37-52.

Miyashiro, A. (1974) Volcanic rock series in island arcs and active continental margins. *Am. J. Sci.*, 274, 321-355.

Nagao, T., Kakubuchi, S. and Shiraki, K. (1997) Determination of major and trace element compositions in rock samples by the automatic X-ray fluorescence spectrometer (Rigaku/RIX3000). *Rep. Center Inst. Anal., Yamaguchi Univ.*, 5, 10-15 (in Japanese).

Nakagawa, H. and Murakami, M. (1975) Geology of Kumejima, Okinawa Gunto, Ryukyu Islands, Japan. *Contrib. Inst. Geol. Paleo., Tohoku Univ.*, 75, 1-16 (in Japanese with English abstract).

Nakamura, Y., Kameo, K., Asahara, Y. and Ozawa, T. (1999) Stratigraphy and geologic age of the Neogene Shimajiri Group on Kumejima Island, Ryukyu Islands. *J. Geol. Soc. Japan*, 105, 757-770 (in Japanese with English abstract).

Nesbitt, H.W. and Wilson, R.E. (1992) Recent chemical weathering of basalts. *Am. J. Sci.*, 292, 740-777.

Perfit, M.R., Gust, D.A., Bence, A.E., Arculus, R.J. and Taylor, A.R. (1980) Chemical characteristics of island-arc basalts: implications for mantle sources. *Chem. Geol.*, 30, 227-256.

Price, R.C., Gray, C.M., Wilson, R.E., Frey, F.A. and Taylor, S.R. (1991) The effects of weathering on rare-earth element, Y and Ba abundances in Tertiary basalts from southeastern Australia. *Chem. Geol.*, 93, 245-265.

Shinjo, R. (1999) Geochemistry of high Mg andesites and the tectonic evolution of the Okinawa Trough-Ryukyu arc system. *Chem. Geol.*, 157, 69-88.

Shinjo, R. and Kato, Y. (1988) Petrography of the Ara-dake Formation, Kume-jima Island, the Ryukyu Islands. *J. Japan. Assoc. Mineral. Petrol. Econ. Geol.*, 85, 282-297 (in Japanese with English abstract).

Shinjo, R., Chung, S.-L., Kato, Y. and Kimura, M. (1999) Geochemical and Sr-Nd isotopic characteristics of volcanic rocks from the Okinawa Trough and Ryukyu Arc: Implications for the evolution of a young, intracontinental back arc basin. *J. Geophys. Res.*, 104, 10591-10608.

Shinjo, R. and Kato, Y. (2000) Geochemical constraints on the origin of bimodal magmatism at the Okinawa Trough, an incipient back-arc basin. *Lithos*, 54, 117-137.

Shinjo, R., Woodhead, J.D. and Hergt, J.M. (2000) Geochemical variation within the northern Ryukyu Arc: magma source compositions and geodynamic implications. *Contrib. Mineral. Petrol.*, 140, 263-282.

Sun, S.-s. and McDonough, W.F. (1989) Chemical and isotopic systematics of oceanic basalts: implications for mantle composition and processes. *In* Magmatism in Ocean Basins (Saunders, A.D. and Norry, M.J. Eds.). pp.398, Geological Society Special Publication, 42, London, 313-345.

Taylor, S.R. and McLennan, S.M. (1995) The geochemical evolution of the continental crust. *Review. Geophys.*, 33, 241-265.

Terakado, Y. and Nakamura, N. (1984) Nd and Sr isotopic variations in acidic rocks from Japan: significance of upper-mantle heterogeneity. *Contrib. Mineral. Petrol.*, 87, 407-417.

Wedepohl, K.H. (1995) The composition of the continental crust. *Geochim. Cosmochim. Acta.*, 59, 1217-1232.